Electronic Supplementary Material (ESI) for CrystEngComm.

Supporting Information

A highly stable Zn coordination polymer exhibiting pH-dependent fluorescence and as a visually ratiometric and on–off fluorescence sensor

Po-Min Chuang and Jing-Yun Wu*

Department of Applied Chemistry, National Chi Nan University, Nantou 545, Taiwan.

E-mail: jyunwu@ncnu.edu.tw

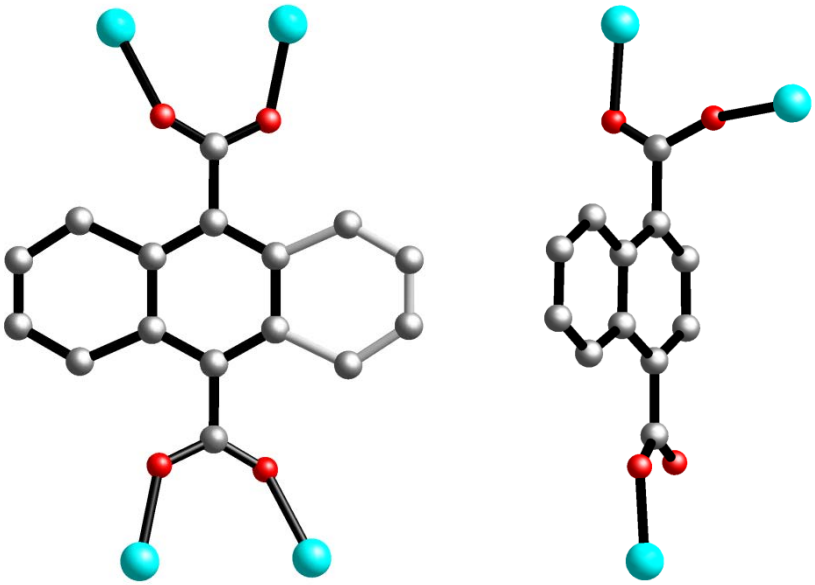

Fig. S1 Coordination modes of 1,4-ndc^{2-} ligand in **1**: (left) the μ_4-bridging mode with two carboxylate groups both in a bidentate syn,syn-bridging mode; (right) the μ_3-bridging mode with one carboxylate group in a monodentate mode and the other one in a bidentate syn,anti-bridging mode.

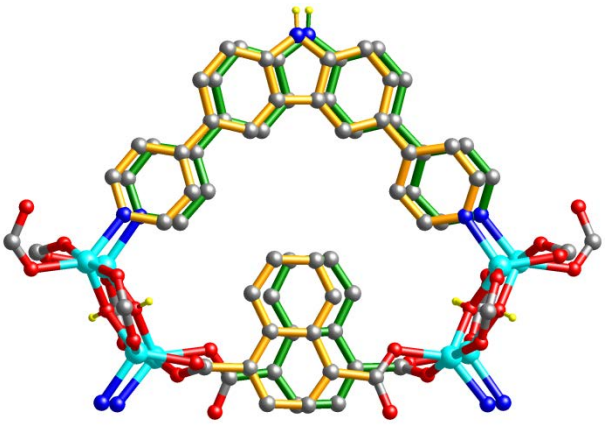

Fig. S2 Perspective view of intramolecular $\pi-\pi$ interactions between two neighboring carbazole moieties and between two neighboring naphthalene moieties in **1**.

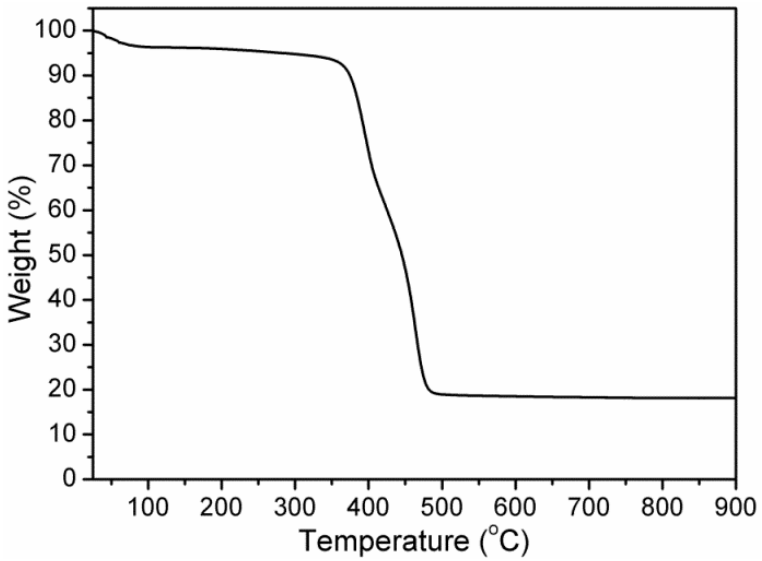

Fig. S3 TG diagram of **1**.

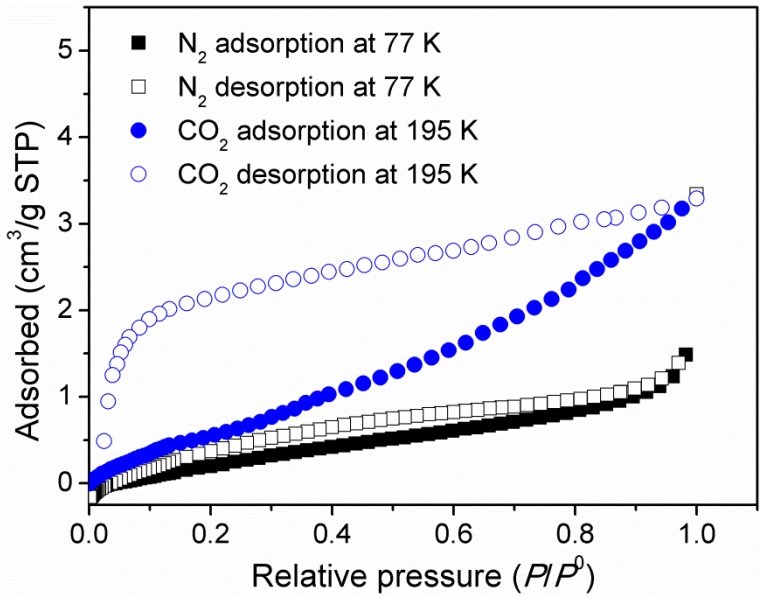

Fig. S4 Low-pressure N_2 and CO_2 adsorption/desorption isotherms of activated **1**.

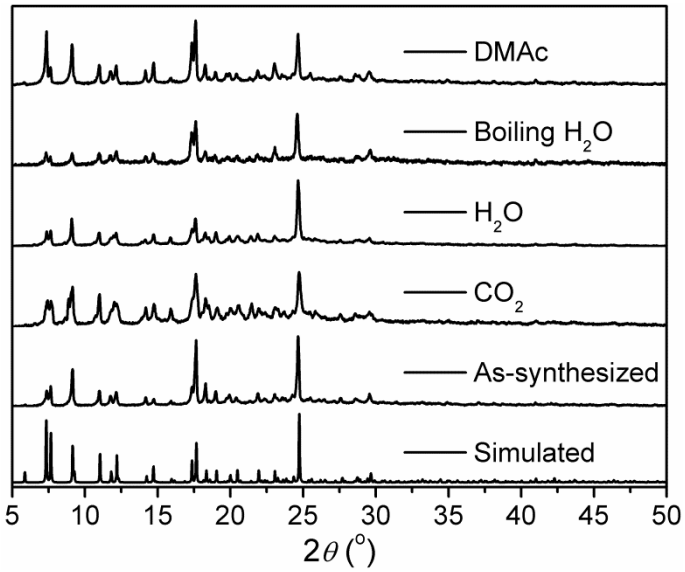

Fig. S5 XRPD patterns of **1**: simulated, as-synthesized, after CO_2 adsorption, and after immersion in H_2O, DMAc at room temperature, and boiling H_2O for 1 day.

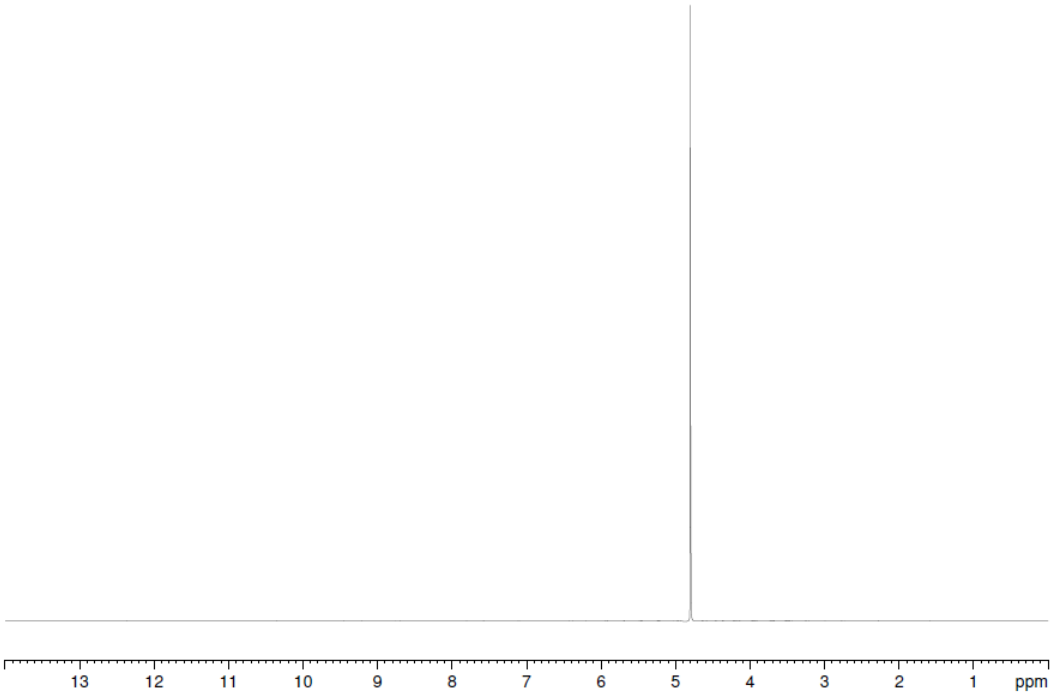

Fig. S6 ^1H NMR spectrum of the supernatant of **1** dispersed in D_2O at room temperature for 1 day.

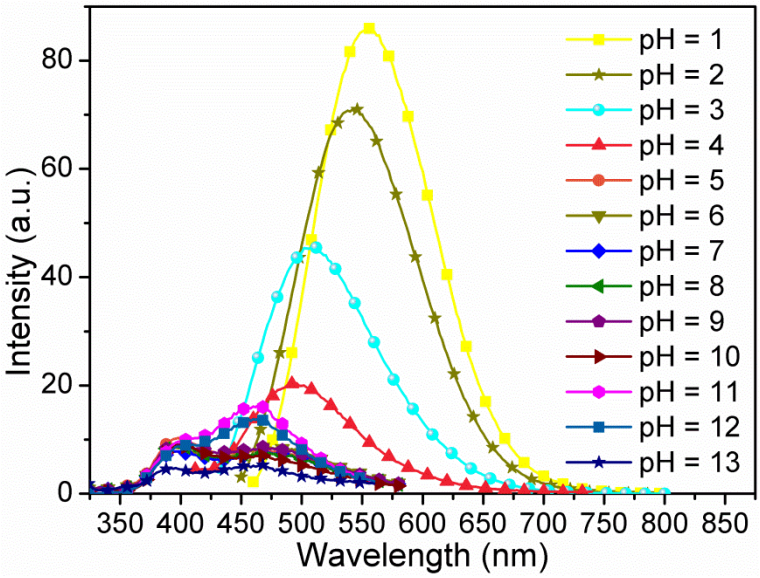

Fig. S7 Fluorescence emission spectra of Cz-3,6-bpy in different pH aqueous solutions ranging from 1 to 13 upon excitation at 350 nm.

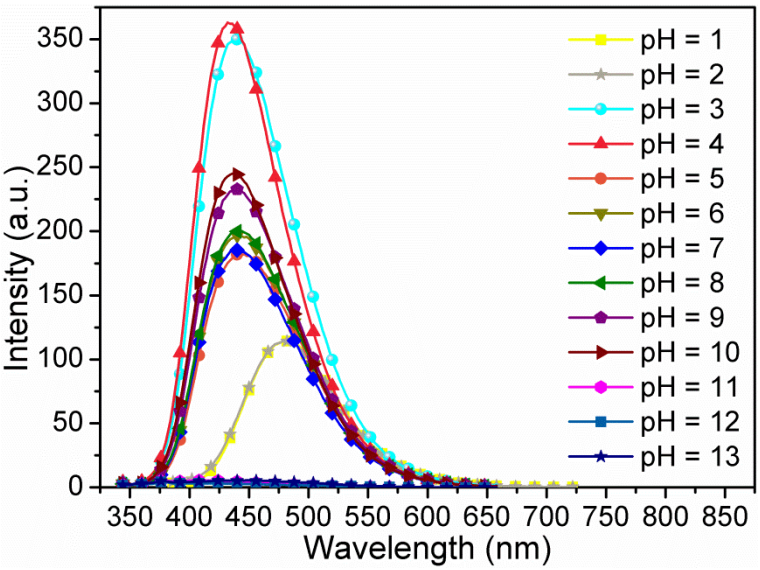

Fig. S8 Fluorescence emission spectra of 1,4-H_2ndc in different pH aqueous solutions ranging from 1 to 13 upon excitation at 350 nm.

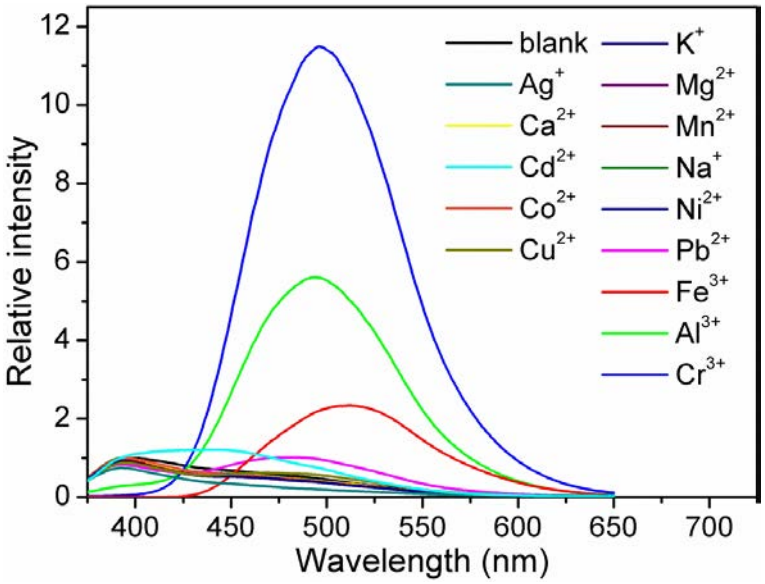

Fig. S9 Fluorescence spectra of free Cz-3,6-bpy ligand in H_2O suspension before and after addition of different metal ions at 1.0 mM upon excitation at 350 nm.

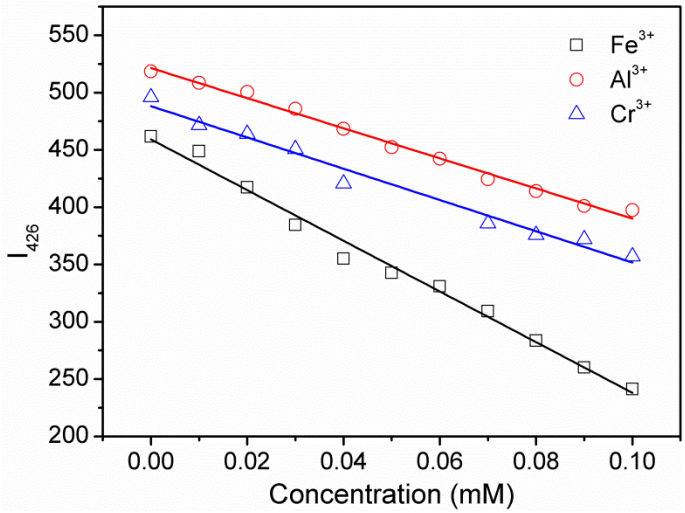

	Fe^{3+}	Al^{3+}	Cr^{3+}
Blank reading 1	466.3	528.0	504.0
Blank reading 2	467.0	527.7	503.3
Blank reading 3	467.4	519.8	498.6
Blank reading 4	471.2	522.6	495.9
Blank reading 5	461.7	518.6	495.9
Standard deviation (σ)	***3.391***	***4.367***	***3.918***
/ Slope / (k), mM^{-1}	***2212***	***1313***	***1365***
R^2	0.98868	0.99092	0.97848
LOD (3σ/k), μM	**4.60**	**9.97**	**8.61**

Fig. S10 Plots of fluorescence intensity of λ = 426 nm (I_{426}) versus metal ion concentration for **1** suspension in H_2O at 0–0.10 mM upon excitation at 350 nm. The following table shows the relevant parameters for LOD calculation for **1** suspension in H_2O toward Fe^{3+}, Al^{3+}, and Cr^{3+} ions.

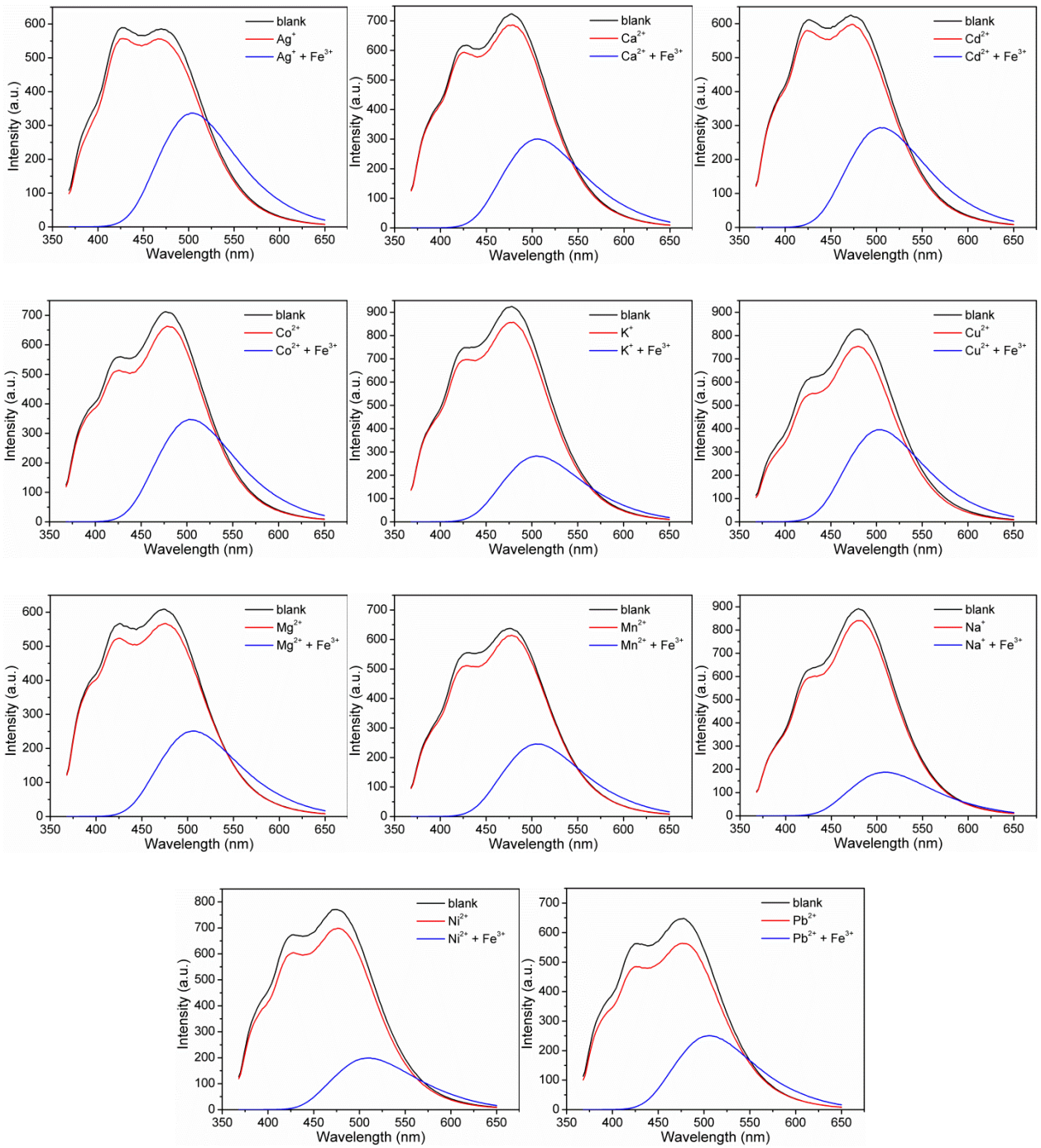

Fig. S11 Fluorescence spectra of **1** suspension in H_2O before and after addition of different interfering metal ions at 1.0 mM and the concomitant addition of the same concentration of Fe^{3+} upon excitation at 350 nm.

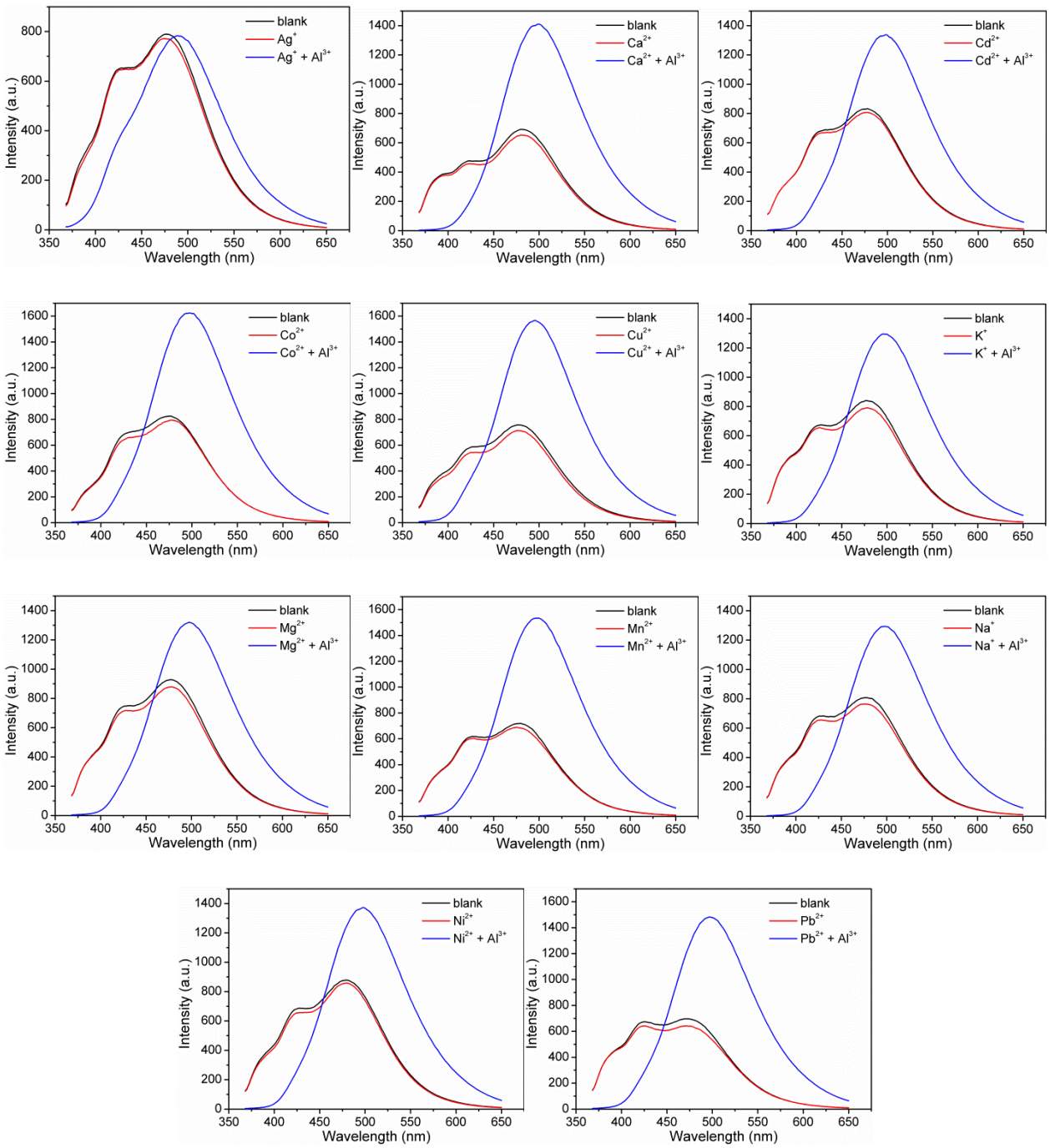

Fig. S12 Fluorescence spectra of **1** suspension in H_2O before and after addition of different interfering metal ions at 1.0 mM and the concomitant addition of the same concentration of Al^{3+} upon excitation at 350 nm.

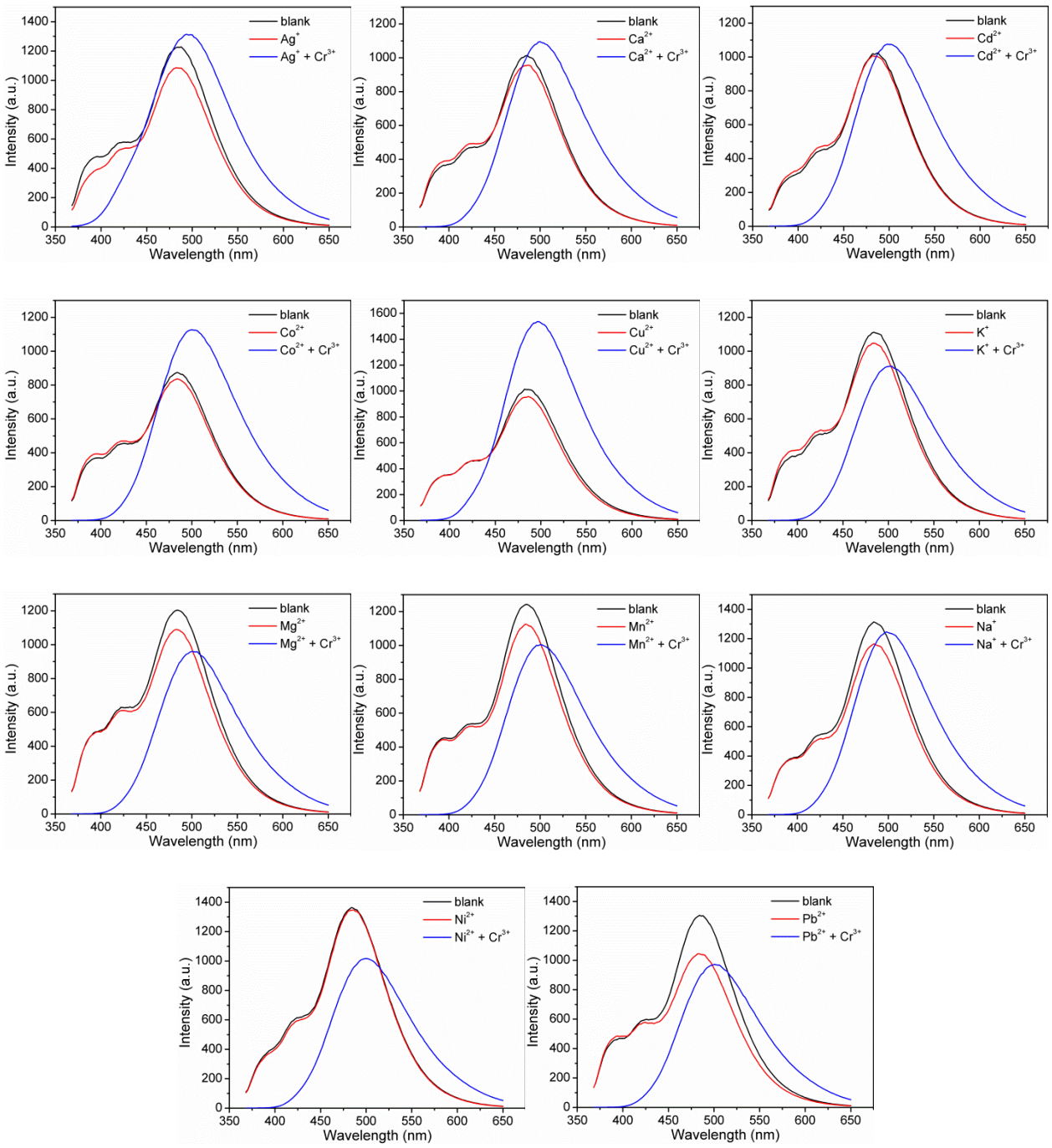

Fig. S13 Fluorescence spectra of **1** suspension in H_2O before and after addition of different interfering metal ions at 1.0 mM and the concomitant addition of the same concentration of Cr^{3+} upon excitation at 350 nm.

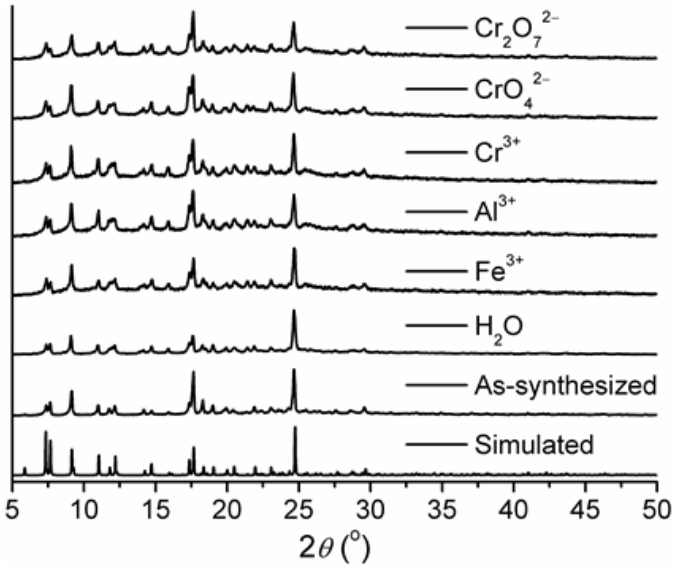

Fig. S14 XRPD patterns of **1** in various situations: simulated, as-synthesized, after immersion in H_2O for 1 day, and after treated with Fe^{3+}, Al^{3+}, Cr^{3+}, CrO_4^{2-}, and $Cr_2O_7^{2-}$ in H_2O for 1 day.

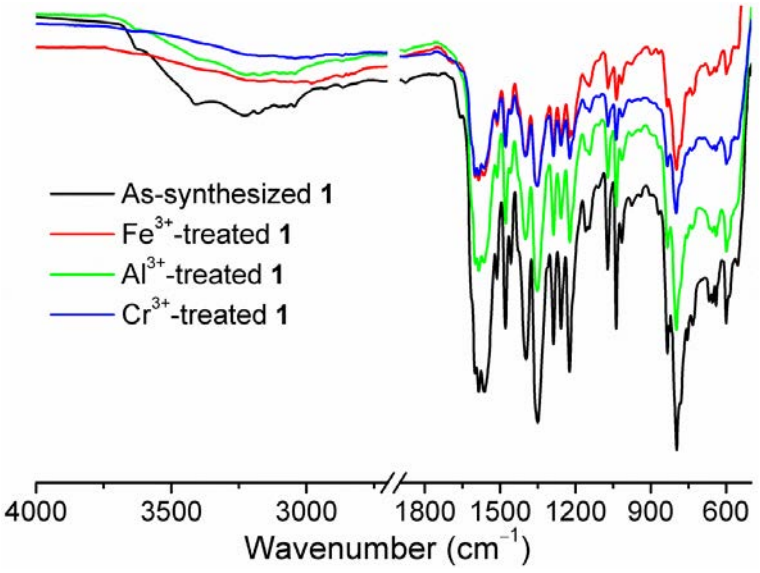

Fig. S15 IR spectra of **1** before and after treated with Fe^{3+}, Al^{3+}, and Cr^{3+} in H_2O for 1 day.

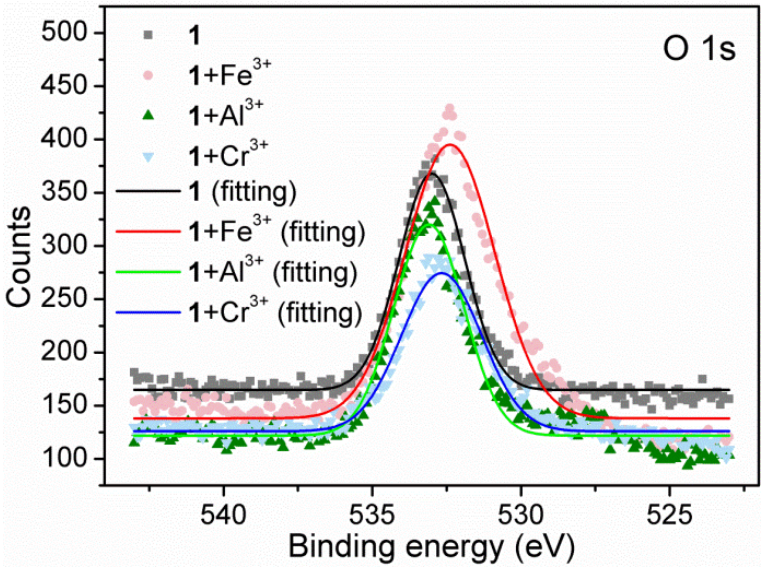

Fig. S16 O 1*s* XPS spectra of as-synthesized **1** and Fe^{3+}-, Al^{3+}-, and Cr^{3+}-treated **1**.

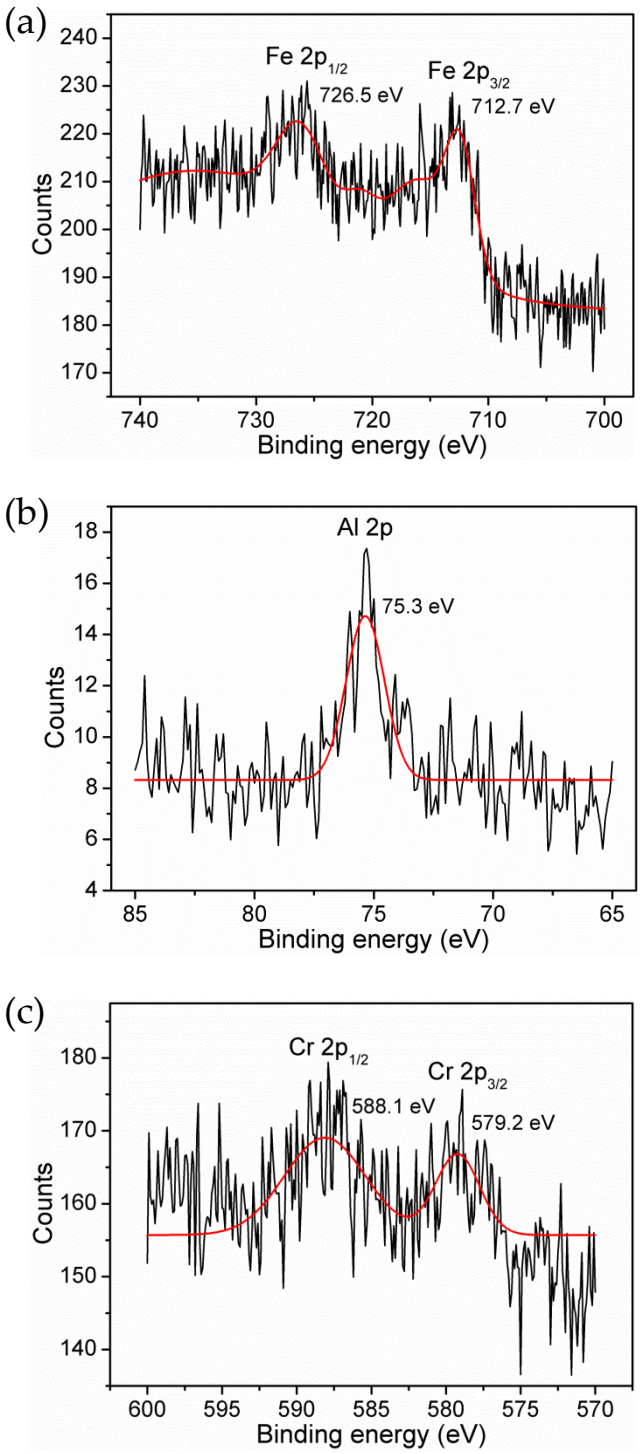

Fig. S17 (a) Fe 2*p* (b) Al 2*p*, and (c) Cr 2*p* XPS spectra of Fe^{3+}-, Al^{3+}-, and Cr^{3+}-treated **1**, respectively.

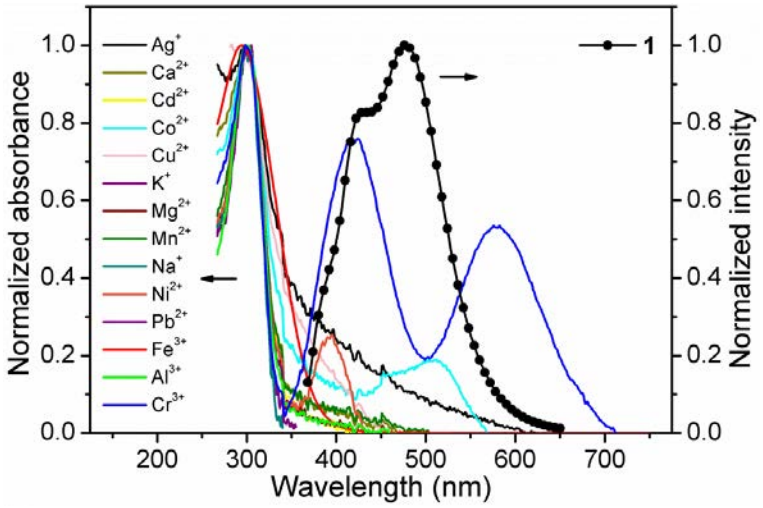

Fig. S18 Spectra overlap between the normalized absorption spectra of all tested metal ions in aqueous solutions and the normalized emission spectra of **1** suspension in H_2O upon excitation at 350 nm.

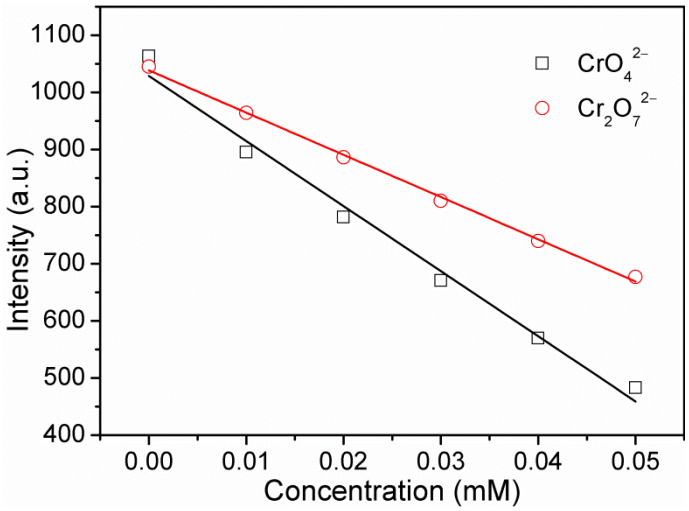

	CrO_4^{2-}	$Cr_2O_7^{2-}$
Blank reading 1	1061	1051
Blank reading 2	1067	1050
Blank reading 3	1063	1039
Blank reading 4	1068	1044
Blank reading 5	1058	1045
Standard deviation (σ)	***4.159***	***4.354***
/ Slope / (k), mM^{-1}	***11394***	***7388***
R^2	0.98478	0.99757
LOD (3σ/k), μM	**1.10**	**1.77**

Fig. S19 Plots of fluorescence intensity versus anion concentration for **1** suspension in H_2O at 0–0.05 mM upon excitation at 350 nm. The following table shows the relevant parameters for LOD calculation for **1** suspension in H_2O toward CrO_4^{2-} and $Cr_2O_7^{2-}$ ions.

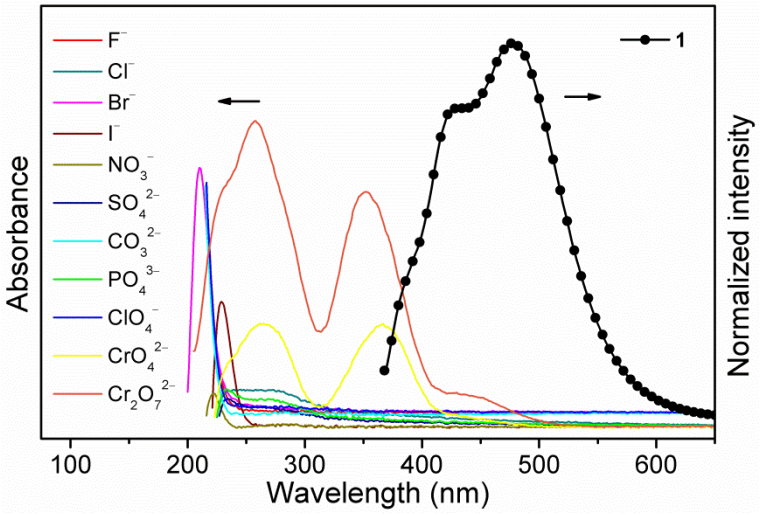

Fig. S20 Spectra overlap between the absorption spectra of all tested anions in aqueous solutions and the normalized emission spectra of **1** suspension in H_2O upon excitation at 350 nm.

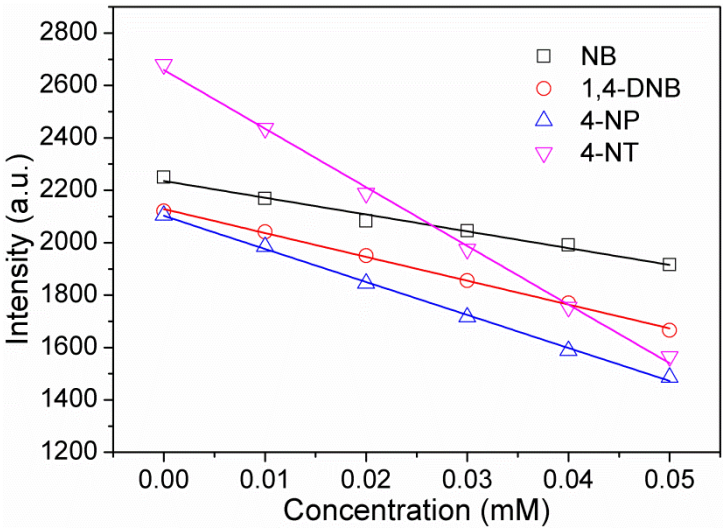

	NB	1,4-DNB	4-NP	4-NT
Blank reading 1	2258	2128	2100	2680
Blank reading 2	2255	2123	2098	2679
Blank reading 3	2252	2126	2104	2684
Blank reading 4	2250	2121	2098	2688
Blank reading 5	2250	2121	2098	2682
Standard deviation (σ)	***3.464***	***3.114***	***2.608***	***3.578***
/ Slope / (k), mM^{-1}	***6397***	***9097***	***12600***	***22382***
R^2	0.98351	0.99849	0.99789	0.99734
LOD (3σ/k), μM	**1.62**	**1.03**	**0.62**	**0.48**

Fig. S21 Plots of fluorescence intensity versus nitroaromatic concentration for **1** suspension in DMAc at 0–0.05 mM upon excitation at 295 nm. The following table shows the relevant parameters for LOD calculation for **1** suspension in DMAc toward various nitroaromatic analytes.

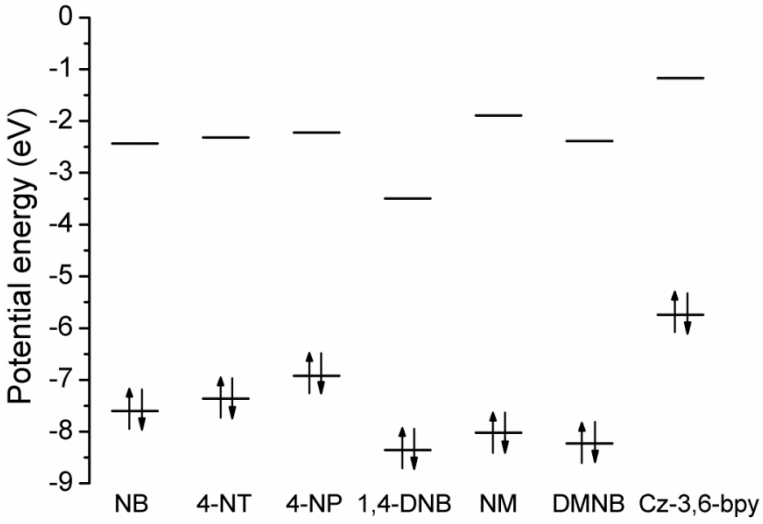

Fig. S22 HOMO and LUMO energies for nitro analytes and Cz-3,6-bpy.

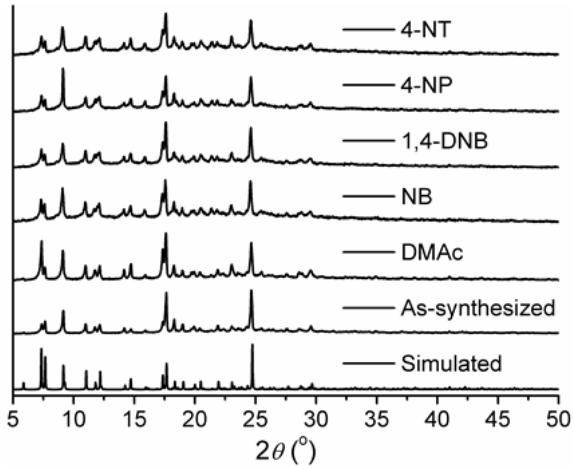

Fig. S23 XRPD patterns of **1** in various situations: simulated, as-synthesized, after immersion in DMAc for 1 day, and after treated with NB, 1,4-DNB, 4-NP, and 4-NT in DMAc for 1 day.

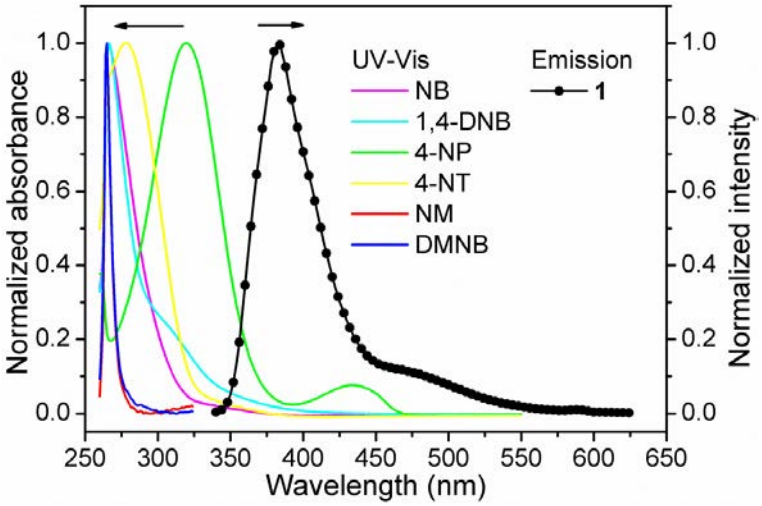

Fig. S24 Spectra overlap between the normalized absorption spectra of all tested nitro compounds in DMAc solutions and the normalized emission spectra of **1** suspension in DMAc upon excitation at 295 nm.